5-1-2000

Interwoven magnetic and flux line structures in single crystal (Tm,Er)Ni2B2C

P. L. Gammel
Lucent Technologies

D. Lopez
Lucent Technologies

D. J. Bishop
Lucent Technologies

M. R. Eskildsen
Risø National Laboratories

N. H. Andersen
Risø National Laboratories

See next page for additional authors

Interwoven magnetic and flux line structures in single crystal (Tm,Er)Ni2B2C

Abstract
We review studies of the interactions between magnetic order and the flux line lattice (FLL) in the (RE)Ni2B2Cintermetallic borocarbides for (RE)=Tm and Er using small angle neutron scattering (SANS) and magneto-transport. For (RE)=Tm the magnetic order and the FLL assume a common symmetry, sharing a phase transition at ~2 kOe, despite an order of magnitude difference in periodicity. For (RE)=Er, the penetration depth λ and the coherence length ξ, both of which are derived from the FLL form factor, are modified near TN=6 K by a theoretically predicted weakly divergent pairbreaking. Finally, below 2.3 K, (RE)=Er shows a coexistence of weak ferromagnetism and superconductivity. This state reveals a highly disordered FLL and a striking increase in the critical current, both arising from the strong ferromagnetic pairbreaking.

Keywords
Physics and Astronomy, Ferromagnetism, Coherence, Coherence theory, Crystal structure, Form factor

Disciplines
Condensed Matter Physics

Comments
The following article is from *Journal of Applied Physics* 87 (2000): 5544, doi:10.1063/1.373399. Posted with permission.

Authors
P. L. Gammel, D. Lopez, D. J. Bishop, M. R. Eskildsen, N. H. Andersen, K. Mortensen, I. R. Fisher, K. O. Cheon, and Paul C. Canfield

Interwoven magnetic and flux line structures in single crystal (Tm,Er)Ni 2 B 2 C (invited)

P. L. Gammel, D. Lopez, D. J. Bishop, M. R. Eskildsen, N. H. Andersen, K. Mortensen, I. R. Fisher, K. O. Cheon , and P. C. Canfield

Citation: Journal of Applied Physics **87**, 5544 (2000); doi: 10.1063/1.373399
View online: http://dx.doi.org/10.1063/1.373399
View Table of Contents: http://scitation.aip.org/content/aip/journal/jap/87/9?ver=pdfcov
Published by the AIP Publishing

Superconductivity R. W. McCallum, Chairman

Interwoven magnetic and flux line structures in single crystal (Tm,Er)Ni_2B_2C (invited)

P. L. Gammel,[a] D. Lopez, and D. J. Bishop
Bell Laboratories, Lucent Technologies, 700 Mountain Avenue, Murray Hill, New Jersey 07974

M. R. Eskildsen, N. H. Andersen, and K. Mortensen
Risø National Laboratories, DK-4000, Roskilde, Denmark

I. R. Fisher, K. O. Cheon, and P. C. Canfield
Ames Laboratory and Department of Physics and Astronomy, Iowa State University, Ames, Iowa 50011

We review studies of the interactions between magnetic order and the flux line lattice (FLL) in the (RE)Ni_2B_2C intermetallic borocarbides for (RE)=Tm and Er using small angle neutron scattering (SANS) and magneto-transport. For (RE)=Tm the magnetic order and the FLL assume a common symmetry, sharing a phase transition at ~2 kOe, despite an order of magnitude difference in periodicity. For (RE)=Er, the penetration depth λ and the coherence length ξ, both of which are derived from the FLL form factor, are modified near $T_N=6$ K by a theoretically predicted weakly divergent pairbreaking. Finally, below 2.3 K, (RE)=Er shows a coexistence of weak ferromagnetism and superconductivity. This state reveals a highly disordered FLL and a striking increase in the critical current, both arising from the strong ferromagnetic pairbreaking. © *2000 American Institute of Physics.* [S0021-8979(00)61908-4]

Materials which would simultaneously exhibit both superconductivity and magnetic order are caught on the horns of a dilemma, as these nominally antagonistic phenomena represent distinct manifestations of long range order. Contrary to this epistemology, over the last twenty years, however, starting[1] with the Rhodium Borides (RE)Rh_4B_4 and the ternary Chevrel phases (RE)$Mo_6(S/Se)_6$ and later culminating[2] with (RE)Ni_2B_2C, where (RE) is a rare earth, it has been repeatedly shown that antiferromagnetism readily coexists with superconductivity. Ferromagnetism and superconductivity have a much trickier negotiation. In the case of $ErRh_4B_4$, for example,[3] once the Er sublattice inclines toward ferromagnetic order, superconductivity exists for only 0.1 K below T_N. Preliminary reports[4] of ferromagnetism and superconductivity in the $Eu_{1.5}Ce_{0.5}RuSr_2Cu_2O_{10}$ system have been plagued by complex synthesis and polycrystalline samples. Hence, the recent confirmation[5,6] that weak ferromagnetism coexists with superconductivity for $T<2.5$ K in single crystal $ErNi_2B_2C$ has generated substantial enthusiasm to pursue detailed studies of this ground state.

A particularly rich vehicle for studying the interplay between superconductivity and magnetism is the (RE)Ni_2B_2C system, which is superconducting for rare earth elements (RE)=Y, Dy, Ho, Er, Tm, and Lu with superconducting transition temperatures T_C as high as 16.6 K and upper critical fields H_{C2} exceeding 10 T. For (RE)=Dy, Ho, Er, and Tm there is an additional magnetic transition temperature T_N associated with ordering of the localized 4*f*-electrons on the rare earth site. The ratio T_N/T_C varies from 0.14 (RE=Tm) to 1.6 (RE=Dy) across the rare earth series,[7] meaning that the salient energy scales for superconductivity and magnetism can be explored in both limits $T_N>T_C$ and $T_C>T_N$.

The crystal structure[8] of the borocarbides is body-centered tetragonal, with space group I4/mmm and comprises alternating sheets of Ni_2B_2 and (RE)C. The electronic properties of the borocarbides are, nonetheless, largely three dimensional, showing only modest anisotropy between the basal plane and the *c* axis. The ability to grow large single crystals using a high temperature flux method[9] enables detailed studies in this system. For the SANS experiments described below, all crystals incorporated isotropically enriched ^{11}B to enhance the penetration of thermal neutrons.

The borocarbides are all strongly type-II superconductors, with κ~5–15. In this case, the mixed state response is dominated by the FLL, an array of magnetic vortices, each carrying one flux quantum $\phi_0=h/2e$. The FLL is a soft structure with a long periodicity, whose symmetry and degree of order are easily influenced. In addition, the structure of a flux line contains information on the two basic length scales for superconductivity, the penetration depth λ through the extent of the field around an individual flux line and the coherence length ξ through the size of the flux line core. From these length scales, one can construct all the critical fields for superconductivity.

The FLL in the borocarbides was imaged and studied using the SANS spectrometer on the cold neutron beamline at the Risø National Laboratory DR3 reactor. The experimental setup is shown schematically in Fig. 1. In a SANS

[a]Electronic mail: plg@lucent.com

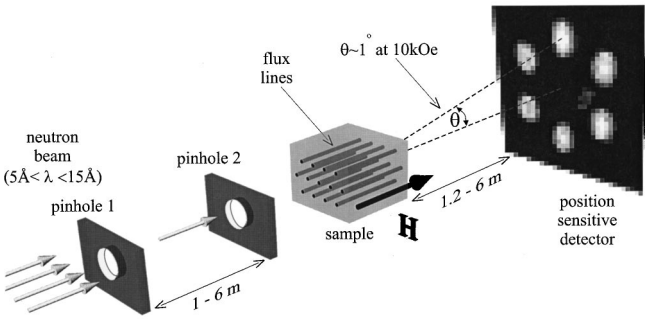

FIG. 1. Schematic diagram of the SANS spectrometer, showing the pinholes used to define the beam divergence and the sample and detector geometry.

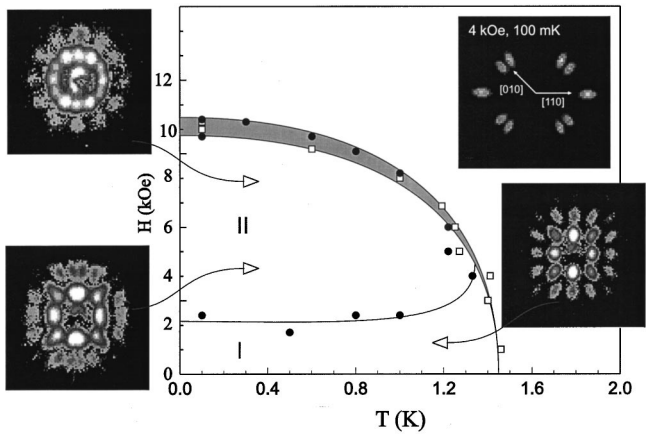

FIG. 2. Shown is the composite FLL and magnetic phase diagram for $TmNi_2B_2C$, with $H\|[001]$, the direction of the ordered moment. In the upper right corner, the inset shows the magnetic diffraction pattern in the SANS geometry. The remaining insets show the FLL diffraction pattern at the fields and temperatures indicated by the arrows.

experiment, the magnetic moment of the neutron is scattered by the spatially varying magnetic field of the flux lines. In the experiments described here, incident neutrons were incident parallel to the applied field. The neutrons had wavelength $\lambda_n = 5-15$ Å, bandwidth $\Delta\lambda_n/\lambda_n = 18\%$ and beam divergence $\sim 0.2°$ defined by the two pinholes. The resulting diffraction pattern was recorded on a position sensitive detector with ~ 5 mm spatial resolution at the end of a 6 m evacuated tank. All measurements were taken following a field cooling procedure, and were subtracted from zero field-cooled data to remove small angle background emanating from the sample and cryostat.

In a SANS experiment, three unique types of data are obtained.[10] First, the structure of the diffraction pattern gives the symmetry of the FLL and its orientation with respect to the host crystal. Second, from the field dependence of the intensity of the lowest order FLL Bragg peaks, one can determine both λ and ξ. For the FLL, the neutron reflectivity can be expressed as $R = (2\pi\gamma_n^2 t/16\phi_0^2 q)H_1^2$, where γ_n is the neutron gyromagnetic ratio and t is the sample thickness. The form factor H_1 has the units of a magnetic field and, using first order Ginzburg–Landau corrections to the London model, is given by $H_1 = (\phi_0/\lambda^2)(1/4\pi^2) \times \exp(-2\pi^2 B\xi^2/\phi_0)$. The length scales λ and ξ were then extracted using this formula and fits to the field dependent reflectivity.

Finally, from the width of the rocking curve, one can extract the FLL longitudinal correlation length ξ_L, a measure of the straightness of the flux lines parallel to the applied field. In principle, analysis of the diffraction peaks in the plane of the detector also allow measurement of the two transverse correlation lengths, but the resolution in this case is typically reduced by a factor of 10–100. Each data type has enhanced our understanding of the interaction between superconductivity and magnetism in the $(RE)Ni_2B_2C$ system, as described below.

$TmNi_2B_2C$ distinguishes itself from other members of the borocarbide family both in regard to the FLL[11] and the magnetic order.[12] For this compound,[13] $T_C = 11.0$ K and $T_N = 1.5$ K. The magnetic order is an incommensurate spin density wave, with wavevector $\mathbf{q} = 0.094(\mathbf{a}^* + \mathbf{b}^*)$. Both the long periodicity of the magnetic order, and the Tm moment direction parallel to c are unique to the Tm compound. This periodicity, ~ 25 Å, can be favorably compared to the superconducting coherence length $\xi \sim 125$ Å, a hint that the two types of order may interact strongly.

Shown in Fig. 2 is the combined magnetic and FLL phase diagram as derived from SANS data. At low fields in region 1, shown in the lower right inset, the FLL is well ordered with the square symmetry ubiquitous[14] in the borocarbide system. As the field is increased, the FLL undergoes a rhombic distortion along the unit cell diagonal, resulting in two domains split by 15° about the crystal [010] direction giving the diffraction pattern in the lower left insert. Finally, as the field is increased above roughly 6 kOe at base temperature, the FLL becomes hexagonal with the unit cell diagonals along [110] as shown in the upper left insert. The reorientation associated with the transition into the hexagonal state means that this cannot be viewed as a continued rhombic distortion, but must be a discontinuous transition. These, as yet unexplained, transitions are coupled to simultaneous changes in the magnetic order.

Because of the long wavelength of the magnetic order, it too can be studied with the SANS spectrometer, simply by reducing λ_n to 2.8 Å and moving the area detector to 1.2 m from the sample. The magnetic scattering is shown in the upper right inset to Fig. 2. In zero applied field, only the peaks along [110] are present. Peaks associated with the second domain, which would lie along the vertical axis, did not satisfy the Bragg condition in this geometry. As with the FLL, the magnetic order is square symmetric. Applying a magnetic field greater than 2 kOe induces a transition in the magnetism, commensurate in field and nature with the FLL transition. Above 2 kOe, the eight peaks split about [010] in the inset appear. The splitting of $\sim 15°$ about [010] is essentially identical to that seen in the FLL. Above 6 kOe, where the FLL shows two domains of hexagonal order, all 12 magnetic peaks show roughly equal intensity, although they retain the symmetry shown in the inset. Above 10 kOe, all magnetic peaks disappear, as the system moves into a saturated paramagnetic state and superconductivity vanishes at H_{C2}. In the main body of Fig. 2, the points represent the principal magnetic transitions.

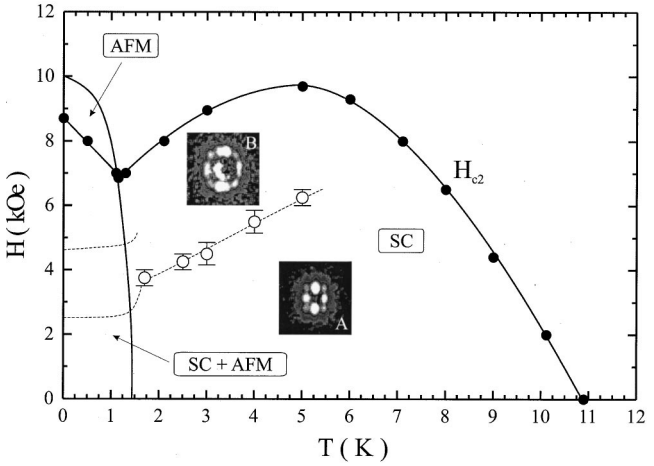

FIG. 3. Shown is the phase diagram for both superconductivity and magnetic order of $TmNi_2B_2C$ over the entire field and temperature range, where AFM denotes spin density wave order and SC denotes superconductivity. Also shown are FLL diffraction patterns indicated that the joint FLL and magnetic transition continues as a FLL transition (○) in the pure SC phase.

This manifestly correlated phase diagram for the FLL and magnetism is shown over the entire temperature range in Fig. 3, where the dashed lines represent FLL data. Two new points emerge from this expanded view. First, the joint FLL and magnetic transition at 2 kOe continues as a sole FLL transition above 1.5 K. This suggests that the FLL is the driving force behind this transition. Second, the proximity of the transition into the saturated paramagnetic state and H_{C2} becomes clear.

Another series of experiments[15] examined hysteresis of the magnetic and FLL symmetry. While the FLL showed no signs of history dependent behavior, there was substantial irreversibility in the magnetic order, as shown in Fig. 4. In this figure, the splitting of the magnetic peaks near the [010] direction is shown. Cooling the samples in a field >10 kOe, followed by a stepwise reduction in the field suppresses the splitting described above. Only when the field is reduced below 4 kOe, i.e., into the rhombohedral FLL phase, does the split reappear. Cooling the sample in zero field, and then raising the field stepwise, results in split magnetic peaks,

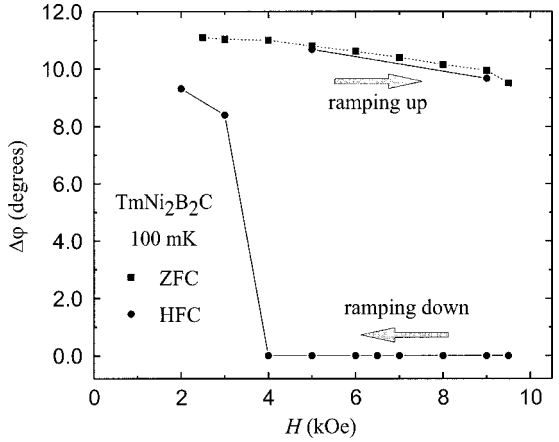

FIG. 4. Shown is the hysteresis of the splitting about [100] of the magnetic diffraction peaks.

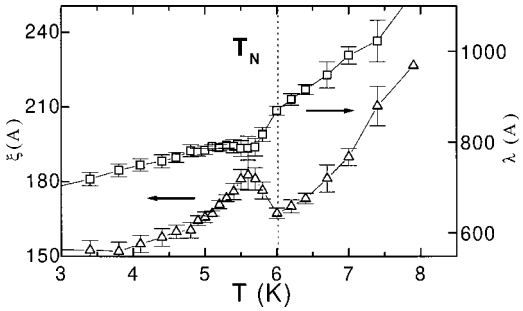

FIG. 5. Shown are the temperature dependence of penetration depth λ (□) and the coherence length (△), as derived from the FLL form factor measured with SANS. Both quantities show distinct features near T_N, indicated by the dotted line.

albeit with a split slightly reduced from what was seen in the field cooled case. This hysteresis, coupled with the stability of the FLL re-enforces the speculation that superconductivity is the driving force behind these field dependent transitions.

Another series of experiments has focused on single-crystal $ErNi_2B_2C$, this time examining λ, ξ (Ref. 16) and the FLL correlation lengths.[10,17] For this system[9] $T_C = 10.5$ K and $T_N = 6.0$ K. The magnetic transition[12] is into an incommensurate transversely polarized spin density wave with $\mathbf{q} = 0.5526\mathbf{a}^*$. Transport data show a pronounced dip in H_{C2} near T_N. In magnetic superconductors, magnetization and specific heat data, which would normally be used to extract λ, H_{C1} and H_C are obscured by the response of the magnetic moments. In particular, the thermodynamic critical field is one of the most fundamental properties of the superconducting state, as it can be related to the energy gap Δ. Hence, SANS provides a unique opportunity to determine these important quantities.

Shown in Fig. 5 are λ and ξ extracted from the flux line form factor as described above. Both parameters show pronounced features near T_N. While both of these can be affected[18] by the gradual 30% increase in the mean free path below T_N and the divergent susceptibility near T_N renormalizes λ, neither of these prosaic explanations fit the data. To understand the impact of these data, the dimensionless Ginzburg–Landau parameter $\kappa = \lambda/\xi$ and the thermodynamic critical field $H_C(T) = \phi_0/[\sqrt{2}\pi\xi(T)\lambda(T)]$ were calculated, the latter using the G–L formula. These data are shown in Fig. 6. The value of κ shows remarkable temperature dependence, dropping more than 20% near T_N, and also assuming a generally lower value in the magnetically ordered state.

Similarly, the data for H_C show a pronounced reduction near T_N. In the inset to Fig. 6, this region is shown on an expanded scale. The dashed line, which accurately described the data in the paramagnetic regime, is the mean field result. Reductions of H_C near T_N have been treated theoretically[19] from the standpoint of pairbreaking. For weak pairbreaking,[20] $H_{C0}/H_C = 1 - 0.57\pi^2\rho$, where H_{C0} denotes the values well away from T_N. For partial Fermi surface nesting, germane to the borocarbides, ρ will contain a weakly divergent contribution $\rho = \rho(T=0) + \Delta\rho[(T-T_N)/T_N]^{\alpha-1}$, where α is the specific heat exponent. This pairbreaking correction is shown as the solid lines in Fig. 6, and provides an excellent fit and explanation of these data.

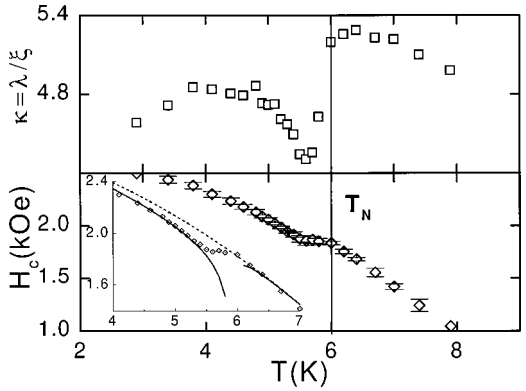

FIG. 6. In the top panel, $\kappa=\lambda/\xi$ is shown. In the lower panel, the thermodynamic critical field H_C is shown, as determined from SANS. In the inset, H_C is expanded near T_N. The dashed line is a mean field fit, while the solid lines include corrections due to the weak divergence of the pairbreaking parameter ρ near T_N.

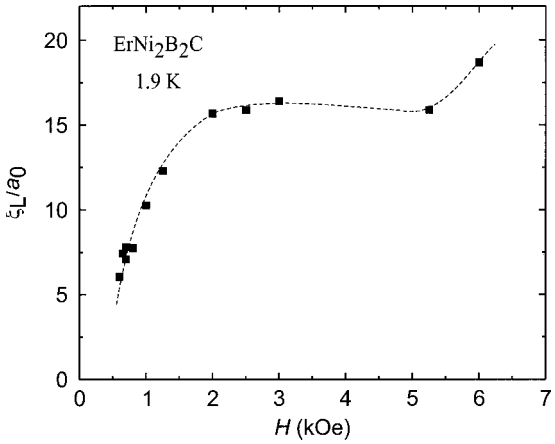

FIG. 7. Shown is the field dependence of longitudinal correlation length, determined from the rocking curve width, of the FLL in $ErNi_2B_2C$ at 1.9 K, below T_{WFM}.

In addition to the coexistence of superconductivity and antiferromagnetism, $ErNi_2B_2C$ exhibits weak ferromagnetism below $T_{\mathrm{WFM}}=2.5$ K. Initial speculations about the existence of this state were based on magnetization data[5] and analogy to $TbNi_2B_2C$.[21] Below 2.5 K, *M-H* loops for $H\|[110]$ and $[100]$ showed a nonzero extrapolation to $H=0$, following the general form of an order parameter and saturating at $\sim 0.3\mu_B$/Er below 2 K. A heuristic argument for this value is based on domain wall ordering in the antiferromagnetic state. The Er spins are approximated as a four position clock model[22] with saturated moment $9\mu_B$/Er, and the modulation $0.553a^*$ can be interpreted as a nearest neighbor antiferromagnet with ferromagnetic domain walls separated by $(0.553-\frac{1}{2})a^*\sim 70$ Å. Were these domain walls, known to be abrupt from the harmonic content of neutron diffraction, to order, a net moment $9\cdot(0.53)\sim 0.4\mu_B$/Er would ensue, similar to what is seen in the data. This result has now been confirmed using spin polarized neutron diffraction, which detects a net moment below 2.5 K.

The nature of the FLL in the state with coexistence of weak ferromagnetism and superconductivity is still unclear. A great deal of excitement has been generated by the prospect of a spontaneously generated FLL in zero applied field.[23] Early SANS data were taken with the field $H\|[001]$, orthogonal to the developing moment. In this case, a slight rotation of the FLL, to accommodate the developing moment, was seen.[10]

More striking, the FLL correlation lengths were dramatically reduced and became field independent as the ferromagnetic state was approached. An example of the field dependent correlation length ξ_L in the ferromagnetic state[24] is shown in Fig. 7. This stands in stark contrast to what is generally observed in type-II superconductors. The straightness of the flux lines, ξ_L, is related[10] to the transport critical J_C current through $\xi_L\approx(B^2/J_C)$. This predicts a correlation length that increases rapidly as a function of field. Generally the product J_CB is constant, leading to $\xi_L\approx B^3$. A cutoff in spatial correlations by strong pairbreaking at the domain walls can be offered as an explanation of the saturation of ξ_L. In general, a consistent picture requires the critical current to increase rapidly both as a function of field and as the temperature is reduced into the ferromagnetic state. Direct measurements of the critical current,[17] using magnetization hysteresis, as shown in Fig. 8 and transport data, have confirmed this unusual behavior.

Over the years, a number of workers have used ferromagnetic impurities, with their concomitant strong pairbreaking, as pinning centers to increase the critical currents in superconducting samples and, in particular, wires.[25] Interpreting those data to isolate the specific role of ferromagnetism from the presence of impurities and defects was made more difficult as the impurity ferromagnetism sets in at a temperature much greater than superconductivity. In $ErNi_2B_2C$ there are two clear advantages in studying the effects of ferromagnetism on superconducting critical current. First and foremost is the $T_{\mathrm{WFM}}(\mathrm{bulk})<T_c(\mathrm{bulk})$, so one can unambiguously see the effect that magnetic order has on pinning and the critical current through studies above and below

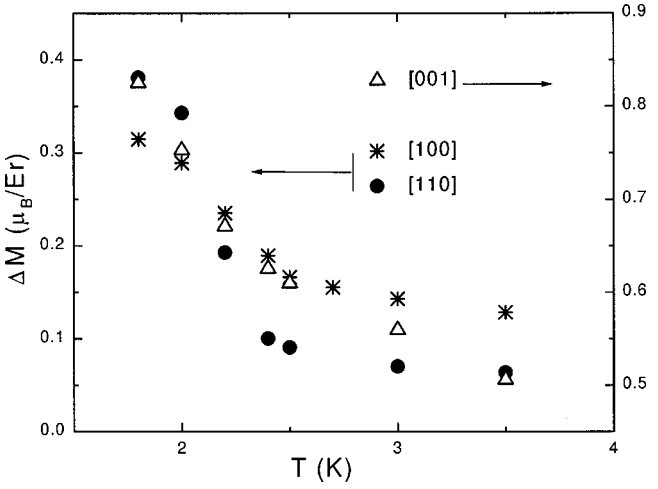

FIG. 8. Shown are the magnetization critical currents $\Delta M\sim J_C$ extrapolated to zero applied field as a function of temperature for three orientations of the magnetic field. Data at other fields follow the same trends, with the rapid increase below $T_{\mathrm{WFM}}\sim 2.5$ K most pronounced for $H\|[110]$. Note: The data for $H\|[001]$ plotted on the right ordinate has an offset zero.

T_{WFM}. Second, in $ErNi_2B_2C$ the ferromagnetism is intrinsic to the material, so the issue of boundary and surface effects is not present.

The $(RE)Ni_2B_2C$ system has proven to be remarkably fertile ground, especially for studies of the interactions between superconductivity and magnetism. The borocarbides have also profoundly impacted other studies of the FLL, including nonlocal effects and symmetry transitions related interactions with the host crystal structure. Until now, studies in this series have been like a new ball of string for a kitten: A wildly entertaining game, batting it around and seeing what happens. Now, the time is ripe to translate this excitement into detailed understanding.

[1] For a review, see *Superconductivity in Ternary Compounds II*, edited by M. B. Maple and Ø. Fischer (Springer-Verlag, Berlin, 1982).
[2] For a review, see P. C. Canfield, P. L. Gammel, and D. J. Bishop, Phys. Today **51**(10), 40 (1998), and references therein.
[3] For a review, see Ø. Fischer, in *Ferromagnetic Materials, Vol. 5*, edited by K. Buschow and E. Wolfarth (Elsevier, Amsterdam, 1990), Chap. 6.
[4] I. Felner and U. Asaf, Physica C **292**, 97 (1997).
[5] P. C. Canfield, S. L. Bud'ko, and B. K. Cho, Physica C **262**, 249 (1996).
[6] H. Kawano, private communication.
[7] B. K. Cho, P. C. Canfield, and D. C. Johnston, Phys. Rev. B **52**, R3844 (1995).
[8] T. Siegrist, H. Zandbergen, R. J. Cava, J. J. Krajewski, and W. F. Peck, Nature (London) **367**, 254 (1994).
[9] B. K. Cho, P. C. Canfield, L. L. Miller, D. C. Johnston, W. P. Beyerman, and A. Yatskar, Phys. Rev. B **52**, 3684 (1995).
[10] U. Yaron, P. L. Gammel, A. P. Ramirez, D. A. Huse, D. J. Bishop, A. I. Goldman, C. Stassis, P. C. Canfield, K. Mortensen, and M. R. Eskildsen, Nature (London) **382**, 236 (1996).
[11] M. R. Eskildsen, K. Harada, P. L. Gammel, A. Abrahamsen, N. Andersen, G. Ernst, A. P. Ramirez, D. J. Bishop, K. Mortensen, D. R. Naugle, K. D. D. Rathnayaka, and P. C. Canfield, Nature (London) **393**, 242 (1998).
[12] J. W. Lynn, S. Skanthakumar, Q. Huang, S. K. Sinha, Z. Hossain, L. C. Gupta, R. Nagarajan, and C. Godart, Phys. Rev. B **55**, 6584 (1997); B. Sternlieb, C. Stassis, A. I. Goldman, P. C. Canfield, and S. Shapiro, J. Appl. Phys. **81**, 4937 (1997).
[13] B. K. Cho, M. Xu, P. C. Canfield, L. L. Miller, and D. C. Johnston, Phys. Rev. B **52**, 3676 (1995).
[14] M. R. Eskildsen, P. L. Gammel, B. P. Barber, A. P. Ramirez, D. J. Bishop, N. H. Andersen, K. Mortensen, C. A. Bolle, C. M. Lieber, and P. C. Canfield, Phys. Rev. Lett. **79**, 487 (1997).
[15] M. R. Eskildsen, K. Harada, P. L. Gammel, N. H. Andersen, G. Ernst, A. P. Ramirez, D. J. Bishop, K. Mortensen, and P. C. Canfield, Physica B **259–261**, 582 (1999).
[16] P. L. Gammel, B. P. Barber, A. P. Ramirez, C. M. Varma, D. J. Bishop, P. C. Canfield, V. G. Kogan, M. R. Eskildsen, N. H. Andersen, K. Mortensen, and K. Harada, Phys. Rev. Lett. **82**, 1756 (1999).
[17] P. L. Gammel, B. P. Barber, A. P. Ramirez, D. J. Bishop, S. L. Bud'ko, and P. C. Canfield, Phys. Rev. Lett. (to be published).
[18] K. E. Gray, Phys. Rev. B **27**, 4157 (1983).
[19] T. V. Ramakrishnan and C. M. Varma, Phys. Rev. B **24**, 137 (1981).
[20] K. Maki, in *Superconductivity*, edited by R. D. Parks (Marcel Dekker, New York, 1969), pp. 1036–1105.
[21] B. K. Cho, P. C. Canfield, and D. C. Johnston, Phys. Rev. B **53**, 8499 (1996); P. Devernagas, J. Zaretsky, C. Stassis, A. I. Goldman, P. C. Canfield, and B. K. Cho, *ibid*. **53**, 8506 (1996).
[22] P. C. Canfield and S. L. Bud'ko, J. Alloys and Compounds **262/263**, 169 (1997).
[23] T. K. Ng and C. M. Varma, Phys. Rev. Lett. **78**, 330 (1997).
[24] M. R. Eskildsen, Ph.D. thesis, http://www.risoe.dk/rispubl/FYS/ris-r-1084.htm.
[25] T. H. Alder and J. D. Livingston, J. Appl. Phys. **37**, 3551 (1966).